Influence of an Epoxy Reactive Diluent on the Thermal Degradation Process of the System DGEBA n = 0/1,2 DCH

Lisardo Núñez, M. Villanueva, M. R. Núñez, B. Rial

Research Group TERBIPROMAT, Departamento de Física Aplicada, Facultade de Física, Universidade de Santiago de Compostela, Campus Sur, 15706, Santiago, Spain

ABSTRACT: The thermal degradation of two epoxy systems diglycidyl ether of bisphenol A (DGEBA n = 0)/1,2-diamine cyclohexane (DCH) containing different concentrations of an epoxy reactive diluent, vinylcyclohexene dioxide (VCHD), was studied by thermogravimetric analysis to determine the reaction mechanism of the degradation process for these two systems. Values of the activation energy, necessary for this study, were calculated by using various integral and differential methods. Values obtained by using the different methods were compared to the value obtained by Kissinger's method, which does not require a knowledge of the reaction mechanism. All the experimental results were compared to master curves in the range of Doyle's approximation (20–35% of conversion). Analysis of the results suggests that the two reaction mechanisms are R_n and F_n deceleratory type in contrast with the sigmoidal A_2 type of the system with filler and the sigmoidal A_4 type of the system without additives. © 2004 Wiley Periodicals, Inc. J Appl Polym Sci 92: 1199–1207, 2004

Key words: thermogravimetry; epoxy resins; epoxy reactive diluent; activation energy; reaction mechanisms

INTRODUCTION

Thermosets are materials with low tensile and storage moduli. For many end uses, it is necessary to add other components to the resin to improve its properties. One of these components is diluents, such as vinylcyclohexene dioxide (VCHD), which do not change significantly the kinetic parameters but vary the mechanical properties, the lifetime, and the thermal degradation kinetics.[1]

Because the behavior of thermosets is affected by the addition of diluents, it is important to investigate the changes taking place during the thermal degradation of these materials. The study of the degradation of a polymer is important because it can determine the upper temperature limit, the mechanism of a solid-state process, and the lifetime for a thermoset.

The main objective of this work was to study the kinetics of thermal degradation of an epoxy resin containing an epoxy reactive diluent (VCHD) in nonisothermal conditions. The results of this study were compared with those of the same epoxy system but without diluent.

Kinetic methods

Thermal gravimetry (TG) nonisothermal experiments register the change of the sample mass as a function of temperature. Kinetic parameters can be extracted from nonisothermal experiments.

The degree of conversion can be expressed as

$$\alpha = \frac{m_0 - m}{m_0 - m_\infty} \tag{1}$$

where m is the measured experimental mass at temperature T, m_0 is the initial mass, and m_∞ is the mass at the end of nonisothermal experiments.

The rate of conversion, $d\alpha/dt$, is a linear function of a temperature-dependent rate constant, k, and a temperature-independent function of conversion, α, that is,

$$\frac{d\alpha}{dt} = kf(\alpha) \tag{2}$$

Substituting Arrhenius equation into eq. (2), one obtains

$$\frac{d\alpha}{dt} = Af(\alpha)e^{(E/RT)} \tag{3}$$

If the temperature of the sample is changed by a controlled and constant heating rate, $\beta = dT/dt$, the variation in the degree of conversion can be analyzed as a function of temperature, this temperature being dependent on the time of heating.

Therefore, the reaction rate gives

TABLE I
Algebraic Expressions for $g(\alpha)$ for the Most Frequently Used Mechanisms of Solid-State Processes

Symbol	$g(\alpha)$	Solid-state processes
	Sigmoidal curves	
A_2	$[-1n(1-\alpha)]^{1/2}$	Nucleation and growth (Avrami eq. 1)
A_3	$[-1n(1-\alpha)]^{1/3}$	Nucleation and growth (Avrami eq. 2)
A_4	$[-1n(1-\alpha)]^{1/4}$	Nucleation and growth (Avrami eq. 3)
	Deceleration curves	
R_1	α	Phase boundary controled reaction (one-dimensional movement)
R_2	$[1-(1-\alpha)^{1/2}]$	Phase boundary controled reaction (contracting area)
R_3	$[1-(1-\alpha)^{1/3}]$	Phase boundary controled reaction (contracting volume)
D_1	α^2	One-dimensional diffusion
D_2	$(1-\alpha)1n(1-\alpha)+\alpha$	Two-dimensional diffusion
D_3	$[1-(1-\alpha)^{1/3}]^2$	Three-dimensional diffusion (Jander equation)
D_4	$(1-2/3\alpha)-(1-\alpha)^{2/3}$	Three-dimensional diffusion (Ginstling–Brounshtein equation)
F_1	$-1n(1-\alpha)$	Random nucleation with one nucleus on the individual particle
F_2	$1/(1-\alpha)$	Random nucleation with two nuclei on the individual particle
F_3	$1/(1-\alpha)^2$	Random nucleation with two nuclei on the individual particle

$$\frac{d\alpha}{dT} = \frac{A}{\beta}e^{(E/RT)}f(\alpha) \qquad (4)$$

Integration of this equation from an initial temperature, T_0, corresponding to a null degree of conversion, to the peak temperature of the derivative thermogravimetric curve (DTG), T_p, where $\alpha = \alpha_p$ gives[2]

$$g(\alpha) = \int_0^{\alpha_p} \frac{d\alpha}{f(\alpha)} = \frac{A}{\beta}\int_0^{T_a} e^{(E/RT)}dT \qquad (5)$$

where $g(\alpha)$ is the integral function of conversion.

In the case of polymers, this integral function, $g(\alpha)$, is either a sigmoidal function or a deceleration function. Table I shows different expressions of $g(\alpha)$ for the different solid-state mechanisms.[3–6] These functions were satisfactorily employed for the estimation of the reaction solid-state mechanism from nonisothermal TG experiments.[7]

Differential method

Analysis of the changes in thermogravimetric data brought about by variations of the heating rate, β, are the basis of the most powerful differential methods for the determination of kinetic parameters. In this article, the Kissinger's method[8] was used.

Integral methods

The integral methods involve an approximate integration of eq. (5). Some of these methods discussed in the present article are Flynn–Wall–Ozawa,[9,10] Coats–Redfern,[11] Van Krevelen,[12] and Horowitz–Metzger.[13]

Criado et al.[4] method for determination of reaction mechanism

The activation energy of a solid-state reaction can be determined from several nonisothermal measurements whatever the reaction mechanism. If the value of the activation energy is known, the kinetic model of the process can be found defining a function

$$Z(\alpha) = \frac{(d\alpha/dt)}{\beta}\Pi(x)T \qquad (6)$$

where $x = E/RT$ and $\Pi(x)$ is an approximation of the temperature integral which cannot be expressed in a simple analytical form. In this study, we used the fourth rational expression of Senum and Yang,[14] which gives errors of lower than 10^{-5}% for $x = 20$.

A combination of eqs. (2) and (6) gives

$$Z(\alpha) = f(\alpha)g(\alpha) \qquad (7)$$

This last equation was used to obtain the master curves as a function of the reaction degree corresponding to the different models listed in Table I.

Plotting the $Z(\alpha)$ function calculated by using both experimental data and eq. (6), and comparing with the master curves, leads to easy and precise determination of the mechanisms of the solid-state processes.

EXPERIMENTAL

Materials

The epoxy resin was a commercial diglycidyl ether of bisphenol A (DGEBA; $n = 0$; Resin 332, Sigma Chemical Co., St. Louis, MO, USA) and the epoxy reactive diluent was VCHD (Fluka, Buchs, Switzerland), with equivalent molecular weights of 173.6 and 71.25 g/Eq,
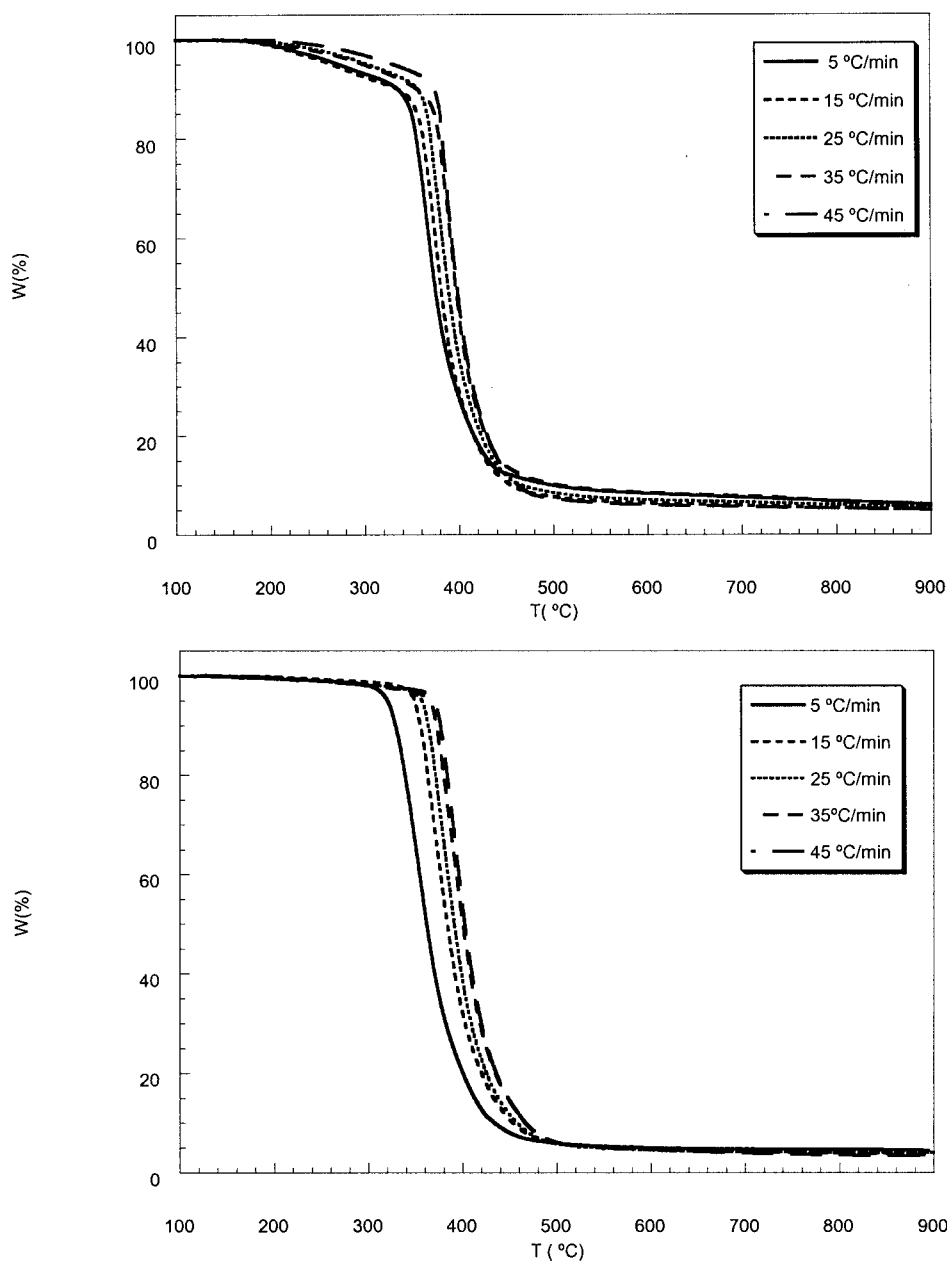
Figure 1 Experimental TG curves at the various heating rates used in this study for the (a) DGEBA ($n = 0$)/1,2 DCH/15% VCHD (nonstoich.) and (b) DGEBA ($n = 0$)/1,2 DCH/15% VCHD (stoich.) systems.

respectively, as determined by wet analysis.[15,16] The curing agent was 1,2-diaminecyclohexane (DCH; Fluka), with an amine hydrogen weight of 28.5.

Sample preparation

Epoxy resin and reactive diluent were carefully and homogeneously mixed, at the proportion in weight of diluent 15% of the total mass of the composed system, before adding the hardener. Then, the amounts of curing agent were added depending on the designed system. For the system noted as 15% VCHD (stoich.),

TABLE II
Inflection Point Temperature at Different Heating Rates

	$T_{\text{inflection point}}$(°C)		
β (°C/min)	0%[21]	15% Nonstoichiometry	15% Stoichiometry
5	343.76	357.51	357.37
15	368.75	378.75	373.75
25	376.25	381.25	373.24
35	383.75	385.00	384.18
45	390.00	386.25	392.00

TABLE III
Residue at 890°C at Different Heating Rates

%VCHD	5°C/min	15°C/min	25°C/min	35°C/min	45°C/min
0	7.60	6.51	7.31	6.13	5.22
15 Nonstoichiometry	5.88	5.00	5.60	5.00	5.00
15 Stoichiometry	4.60	4.42	4.06	3.63	3.37

a stoichiometric amount of curing agent was added, taking into account the excess of epoxy introduced by the diluent. For the system noted as 15% VCHD (nonstoich.), the epoxy excess introduced by the reactive diluent was not taken into account, so it was not compensated. Finally, the sample was introduced in a cylindrical frame.

For these 15% VCHD (stoich.) and 15% VCHD (nonstoich.) systems, the curing reactions were programmed according to the TTT diagrams calculated in our premises for the DGEBA ($n = 0$)/1,2 DCH/15% VCHD stoichiometric system and for the DGEBA ($n = 0$)/1,2 DCH system,[17] respectively.

These curing reactions were 35 min at 120°C in a stove for the 15% VCHD (stoich.); or a first step 24 h at 23°C and a second one 16 h at 70°C in a stove, for the 15% VCHD (nonstoich.).

For thermogravimetric analysis, the samples were cut in the form of 15–25 mg in weight and 6 mm in diameter discs.

Thermogravimetric analysis was performed by using a thermogravimetric analyzer (TGA7) from Perkin–Elmer controlled by a 1020 computer. This microbalance was calibrated making use of the discontinuous change in the magnetic properties of perkalloy and alumel on heating. The Curie point of each alloy was calculated by the microbalance which was calibrated at different heating rates.

The system was operated in the dynamic mode in the temperature range 100–900°C, at different heating rates of 5, 15, 25, 35, and 45°C/min.

All the experiments were carried out under a dry nitrogen atmosphere. The TGA7 analyzer requires two purge lines: one to purge the balance chamber and a second one to purge the sample-furnace area. After various experiments, it was found that the optimum gas flow rates were 25 mL/min for the balance purge gas and 35 mL/min for the sample purge gas.

RESULTS AND DISCUSSION

Figure 1(a, b) shows the thermal degradation curves corresponding to dynamic experiments carried out at different heating rates (5, 15, 25, 35, and 45°C/min), for the nonstoichiometric and stoichiometric systems, respectively. These curves are C-type,[4] which correspond to a one-stage decomposition reaction where the procedural decomposition temperatures (initial

and final) are well defined. The step is due to the thermal degradation of the epoxy resin. The inflection point temperature corresponding to the first step, T_m, can be determined from the minimum of the derivative of these curves, and the residual mass can be measured from these TG curves after complete degradation. Tables II and III show the inflection point temperatures of the first step, T_m, and the residual mass, at different heating rates, respectively, for the system without diluent, the nonstoichiometric, and the stoichiometric. Analysis of Table II shows that the inflection temperatures are very similar for the three epoxy systems: the differences being within the 5% of error allowed by the IUPAC. However, there are significant differences in the residue values. The highest values correspond to the system without diluent and the lowest values were obtained for the system with the stoichiometric ratio of diluent. It can be seen that, in all the cases, the residual mass is nearly independent of the heating rate.

Owing to the thermodegradation behavior of the epoxy systems here studied, we have chosen 10°C/min heating rate intervals, instead of 5°C/min intervals used by some authors,[18,19] to avoid the overlapping of inflection point temperatures. This same procedure was followed in the study of the epoxy system without filler.

By using the Kissinger equation[8] and the inflection point temperature corresponding to the thermograms shown in Figure 1, the activation energies were calcu-

TABLE IV
Activation Energies Obtained Using Flynn–Wall–Ozawa Method

α	%VCHD	$E_a \pm s(E_a)$ (kJ mol^{-1})	R
0.20	15 Nonstoichiometry	201.10 ± 14.55	0.9922
	15 Stoichiometry	157.91 ± 6.70	0.9973
0.23	15 Nonstoichiometry	206.70 ± 14.01	0.9932
	15 Stoichiometry	161.01 ± 7.13	0.9971
0.26	15 Nonstoichiometry	212.38 ± 14.19	0.9934
	15 Stoichiometry	164.39 ± 7.61	0.9968
0.29	15 Nonstoichiometry	217.20 ± 14.01	0.9938
	15 Stoichiometry	166.94 ± 8.14	0.9964
0.32	15 Nonstoichiometry	219.95 ± 13.28	0.9946
	15 Stoichiometry	169.34 ± 8.78	0.9960
0.35	15 Nonstoichiometry	222.64 ± 13.64	0.9944
	15 Stoichiometry	171.97 ± 9.34	0.9956

TABLE V
**Activation Energies Obtained Using Coats–Redfern
Method for Several Solid-State Processes at a Heating
Rate of 5°C/min**

Mechanism	15% VCHD Nonstoich.		15% VCHD Stoich.	
	E_a (kJ mol^{-1})	R	E_a (kJ mol^{-1})	R
A_2	101.50	0.9993	97.53	0.9985
A_3	64.12	0.9993	61.47	0.9984
A_4	45.42	0.9992	43.45	0.9981
R_1	180.16	0.9987	173.36	0.9977
R_2	196.43	0.9991	189.08	0.9982
R_3	202.07	0.9992	194.53	0.9984
D_1	370.97	0.9979	357.38	0.9978
D_2	392.05	0.9988	377.75	0.9985
D_3	414.79	0.9990	399.72	0.9985
D_4	399.61	0.9993	385.07	0.9983
F_1	213.66	0.9991	205.73	0.9987
F_2	60.17	0.9994	57.77	0.9984
F_3	130.99	0.9967	136.42	0.9988

TABLE VII
**Activation Energies Obtained Using Coats–Redfern
Method for Several Solid-State Processes at a Heating
Rate of 25°C/min**

Mechanism	15% VCHD Nonstoich.		15% VCHD Stoich.	
	E_a (kJ mol^{-1})	R	E_a (kJ mol^{-1})	R
A_2	116.23	0.9964	107.95	0.9974
A_3	73.89	0.9960	68.37	0.9971
A_4	52.73	0.9956	48.58	0.9967
R_1	205.16	0.9952	191.11	0.9963
R_2	223.66	0.9960	208.39	0.9970
R_3	230.07	0.9962	214.38	0.9972
D_1	421.10	0.9954	393.02	0.9965
D_2	445.07	0.9959	415.41	0.9969
D_3	470.93	0.9964	439.54	0.9974
D_4	453.66	0.9961	423.45	0.9971
F_1	243.25	0.9967	226.69	0.9976
F_2	69.77	0.9993	64.44	0.9994
F_3	150.32	0.9994	149.98	0.9995

lated from a plot of $\ln(\beta/T_{\max}^2)$ versus $1000/T_{\max}$ and fitting to a straight line. The activation energies obtained by using this method were 237.61 ± 36.83 and 211.60 ± 37.99 kJ/mol, for the nonstoichiometric and stoichiometric systems, respectively. Both values are within the confidence interval and are greater than the value (144.01 ± 17.69 kJ/mol) calculated for the system without diluent.[20]

The activation energy can also be determined by using the method of Flynn–Wall–Ozawa,[9,10] from a linear fitting of $\ln \beta$ versus $1000/T$ at different conversions. Owing to the fact that this equation was derived by using the Doyle approximation,[21] only conversion values in the range of 5–35% were used. For the present study, we have used conversion values 20, 23,

26, 29, 32, and 35%. Activation energies corresponding to the different conversions are listed in Table IV. These activation energy values give mean values of 213.33 ± 6.10 and 165.26 ± 9.57 kJ/mol for the non-stoichiometric and stoichiometric systems, respectively.

Compared to others, these two methods present the advantage that they do not require the previous knowledge of the reaction mechanism for determining the activation energy. Some authors[5,18] used the activation energies obtained by using these two methods to check their thermodegradation mechanism models. In this work, the Flynn–Wall–Ozawa energy values were considered as references to compare with those obtained through the different integral methods cited

TABLE VI
**Activation Energies Obtained Using Coats–Redfern
Method for Several Solid-State Processes at a Heating
Rate of 15°C/min**

Mechanism	15% VCHD Nonstoich.		15% VCHD Stoich.	
	E_a (kJ mol^{-1})	R	E_a (kJ mol^{-1})	R
A_2	101.50	0.9993	97.53	0.9985
A_3	64.12	0.9993	61.47	0.9984
A_4	45.42	0.9992	43.45	0.9981
R_1	180.16	0.9987	173.36	0.9977
R_2	196.43	0.9991	189.08	0.9982
R_3	202.07	0.9992	194.53	0.9984
D_1	370.97	0.9979	357.38	0.9978
D_2	392.05	0.9988	377.75	0.9985
D_3	414.79	0.9990	399.72	0.9985
D_4	399.61	0.9993	385.07	0.9983
F_1	213.66	0.9991	205.73	0.9987
F_2	60.17	0.9994	57.77	0.9984
F_3	130.99	0.9967	136.42	0.9988

TABLE VIII
**Activation Energies Obtained Using Coats–Redfern
Method for Several Solid-State Processes at a Heating
Rate of 35°C/min**

Mechanism	15% VCHD Nonstoich.		15% VCHD Stoich.	
	E_a (kJ mol^{-1})	R	E_a (kJ mol^{-1})	R
A_2	120.43	0.9980	106.21	0.9972
A_3	76.68	0.9978	67.16	0.9969
A_4	54.80	0.9975	47.62	0.9965
R_1	212.40	0.9970	188.28	0.9961
R_2	231.48	0.9976	205.33	0.9968
R_3	238.09	0.9978	211.24	0.9970
D_1	435.61	0.9972	387.52	0.9963
D_2	460.34	0.9976	409.62	0.9968
D_3	487.00	0.9979	433.45	0.9972
D_4	469.20	0.9977	417.55	0.9969
F_1	251.68	0.9981	223.40	0.9975
F_2	72.24	0.9984	63.29	0.9994
F_3	155.31	0.9986	148.04	0.9996

TABLE IX
Activation Energies Obtained Using Coats–Redfern Method for Several Solid-State Processes at a Heating Rate of 45°C/min

Mechanism	15% VCHD Nonstoich.		15% VCHD Stoich.	
	E_a (kJ mol^{-1})	R	E_a (kJ mol^{-1})	R
A_2	159.71	0.9965	120.54	0.9986
A_3	102.83	0.9963	76.70	0.9984
A_4	74.38	0.9960	54.77	0.9982
R_1	279.19	0.9953	212.74	0.9977
R_2	304.06	0.9961	231.85	0.9982
R_3	312.68	0.9963	238.47	0.9984
D_1	569.35	0.9955	436.47	0.9978
D_2	601.56	0.9960	461.23	0.9981
D_3	636.31	0.9965	487.94	0.9985
D_4	613.12	0.9961	470.12	0.9983
F_1	330.39	0.9968	252.09	0.9987
F_2	97.31	0.9997	72.21	0.9985
F_3	205.57	0.9998	165.88	0.9899

before. The Flynn–Wall–Ozawa results were considered because the Kissinger method takes only one point of the thermodegradation curve, whereas the Flynn–Wall–Ozawa method takes different points corresponding to different conversion values.

By using the equation proposed by Coats and Redfern,[11] the activation energy for every $g(\alpha)$ listed in Table I can be obtained at constant heating rates from fitting of $\ln[g(\alpha)/T^2]$ versus $1000/T$ plots. For this study, we have used the same conversion values as those used in the previous methods. Tables V–IX show activation energies and correlations for values in the range 5–35% at constant heating rate values of 5, 15, 25, 35, and 45°C/min, respectively. Analysis of these tables show that, at all the heating rate values and for the two systems with diluent, the activation energies in better agreement with those obtained using the Flynn–Wall–Ozawa method correspond to R_n and F_n type mechanisms. These facts suggest that the solid-state thermodegradation mechanism followed by our epoxy systems are deceleratory type, whereas for the system without diluent,[20] the solid-state thermodegradation mechanism was a sigmoidal-type (A_4).

To confirm this deceleratory behavior, we have calculated activation energies and correlations by using Van Krevelen[12] and Horowitz–Metzger[13] models. The

TABLE X
Activation Energies Obtained Using Van Krevelen Method for R_n and F_n Solid-State Processes at Different Heating Rates

β (°C/min)	Mechanism	15% VCHD Nonstoich.		15% VCHD Stoich.	
		E_a (kJ mol^{-1})	R	E_a (kJ mol^{-1})	R
5	R_1	180.68	0.9994	149.25	0.9983
	R_2	196.52	0.9996	162.44	0.9987
	R_3	202.00	0.9997	167.01	0.9989
	F_1	213.28	0.9998	176.41	0.9991
	F_2	63.67	0.9969	52.17	0.9985
	F_3	132.59	0.9969	109.59	0.9985
15	R_1	188.69	0.9988	180.29	0.9978
	R_2	205.25	0.9991	196.16	0.9989
	R_3	210.98	0.9992	201.65	0.9989
	F_1	222.77	0.9994	212.95	0.9987
	F_2	66.65	0.9979	63.68	0.9989
	F_3	138.72	0.9979	132.75	0.9989
25	R_1	212.44	0.9955	195.63	0.9965
	R_2	231.11	0.9962	212.83	0.9971
	R_3	237.58	0.9964	218.79	0.9973
	F_1	250.89	0.9968	231.06	0.9977
	F_2	75.85	0.9995	69.54	0.9996
	F_3	157.14	0.9995	144.46	0.9996
35	R_1	218.98	0.9977	193.05	0.9963
	R_2	238.16	0.9979	210.05	0.9970
	R_3	244.81	0.9972	215.93	0.9972
	F_1	258.48	0.9989	228.04	0.9975
	F_2	78.09	0.9989	68.54	0.9996
	F_3	161.62	0.9989	142.54	0.9996
45	R_1	284.80	0.9955	219.44	0.9978
	R_2	309.68	0.9962	238.67	0.9983
	R_3	318.31	0.9965	245.32	0.9984
	F_1	336.03	0.9969	259.02	0.9987
	F_2	102.85	0.9998	78.16	0.9990
	F_3	211.18	0.9998	161.85	0.9990

TABLE XI
Activation Energies Obtained Using Horowitz–Metzger Method for R_n and F_n Solid-State Processes at Different Heating Rates

β (°C/min)	Mechanism	15% VCHD Nonstoich.		15% VCHD Stoich.	
		E_a (kJ mol^{-1})	R	E_a (kJ mol^{-1})	R
5	R_1	187.89	0.9993	157.22	0.9982
	R_2	203.90	0.9996	170.64	0.9986
	R_3	209.45	0.9996	175.29	0.9987
	F_1	220.85	0.9997	184.86	0.9990
	F_2	69.67	0.9971	58.44	0.9986
	F_3	139.33	0.9971	116.89	0.9986
15	R_1	197.46	0.9986	187.32	0.9976
	R_2	214.31	0.9990	203.34	0.9982
	R_3	220.14	0.9991	208.88	0.9983
	F_1	232.14	0.9993	220.29	0.9986
	F_2	73.33	0.9981	69.70	0.9990
	F_3	146.66	0.9981	139.40	0.9990
25	R_1	219.85	0.9953	200.11	0.9963
	R_2	238.69	0.9960	217.24	0.9970
	R_3	245.22	0.9963	223.18	0.9972
	F_1	258.64	0.9967	235.39	0.9975
	F_2	82.04	0.9995	74.60	0.9996
	F_3	164.08	0.9995	149.20	0.9996
35	R_1	228.20	0.9970	197.78	0.9961
	R_2	247.71	0.9976	214.72	0.9968
	R_3	254.47	0.9978	220.58	0.9970
	F_1	268.38	0.9981	232.65	0.9974
	F_2	84.96	0.9990	73.75	0.9997
	F_3	169.91	0.9990	147.50	0.9997
45	R_1	290.40	0.9953	226.21	0.9976
	R_2	315.30	0.9961	245.54	0.9982
	R_3	323.92	0.9963	252.24	0.9983
	F_1	341.66	0.9967	266.03	0.9986
	F_2	108.40	0.9998	84.17	0.9991
	F_3	216.79	0.9998	168.34	0.9991

Van Krevelen activation energy was obtained through a linear fitting of log α versus log T plots. Table X shows activation energies and correlation values for R_n and F_n mechanisms by using the Van Krevelen model, at different constant heating rate values, for the two systems with diluent.

Table XI shows activation energies and correlations obtained by using R_n and F_n mechanisms and the Horowitz and Metzger model[13] that uses ln $g(\alpha)$ versus $(T - T_r)$ plots. The use of these two methods confirms that the thermodegradation mechanisms followed by the epoxy systems studied are R_n or F_n type but it does not supply further information about a particular mechanism.

Finally, to corroborate that our epoxy systems follow a deceleratory thermodegradation mechanism, we have used the method proposed by Criado et al. This method uses reference theoretical curves called master plots, which are compared to experimental data. Experimental results were obtained from eq. (6) at the heating rates of 35 and 45°C/min.

Figure 2(a, b) shows master curves and experimental results corresponding to the systems with diluent,

at heating rates of 35 and 45°C min^{-1}, respectively. As expected, experimental results depend on the heating rate. This fact is more pronounced for the system with nonstoichiometric diluent proportion. Figure 2(a) suggests that the mechanisms better describing the thermodegradation behavior of both stoichiometric and nonstoichiometric systems at 35°C/min correspond to R_2, R_3, or F_1. However, Figure 2(b) shows that at 45°C/min both systems show differences in their thermodegradation behavior, as the nonstoichiometric system follows a F_3 type, whereas the mechanism followed by the stoichiometric system is not well defined.

Analysis of Table XI shows that the activation energies obtained by using the different methods, at 35 and 45°C/min, are very different from those corresponding to a F_1 mechanism that, because of this, should be rejected.

These results suggest that the thermodegradation kinetics followed by the systems studied correspond to a decelerated-type solid-state mechanism (R_2, R_3, or F_3). At the same time, the thermodegradation behavior depends on the heating rate.
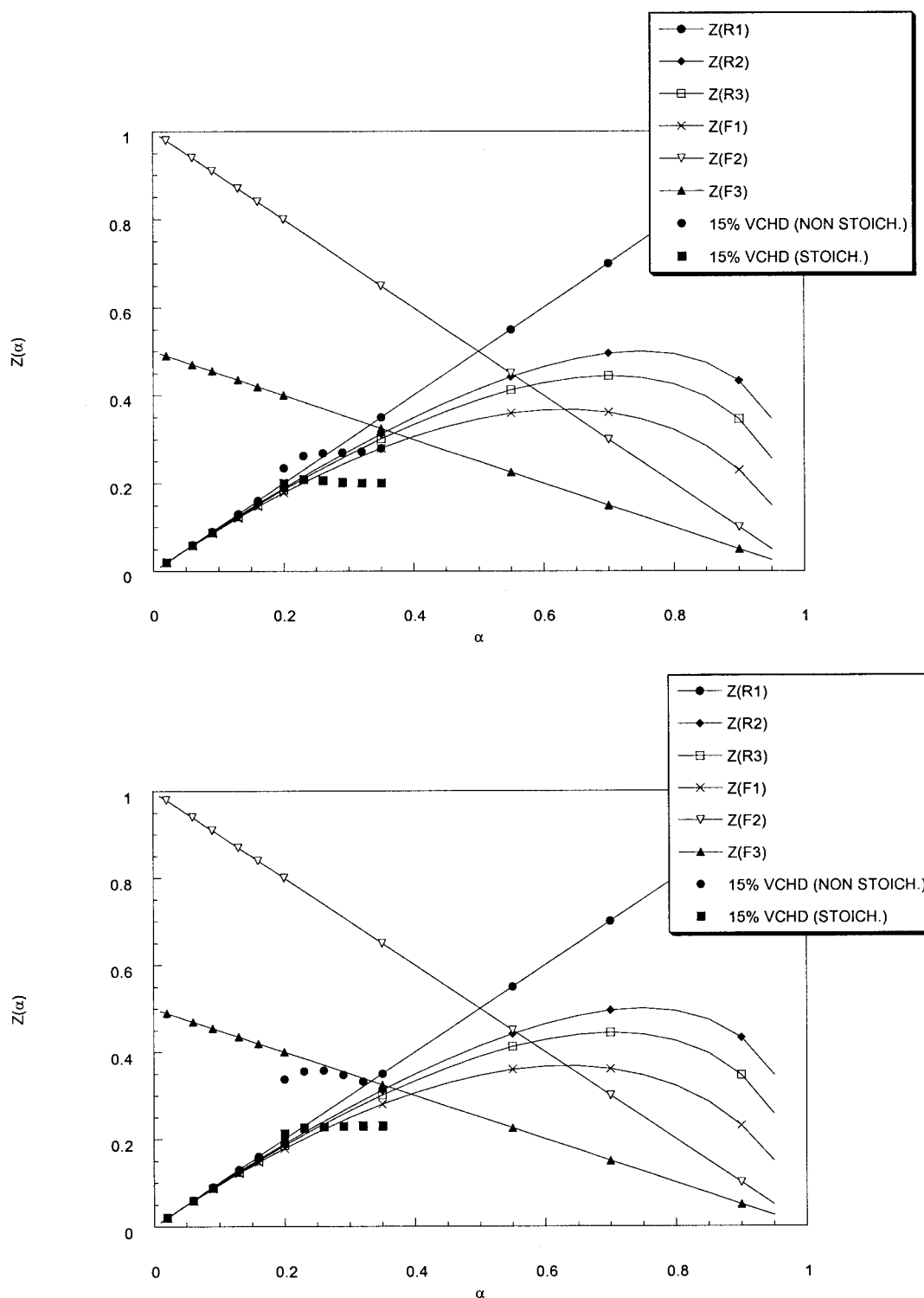
Figure 2 Master curve plots $Z(\alpha)$ versus α, for the DGEBA ($n = 0$)/1,2 DCH/15% VCHD (nonstoich.) and DGEBA ($n = 0$)/1,2 DCH/15% VCHD (stoich.) systems, (a) at 35°C/min and (b) 45°C/min.

CONCLUSION

The thermodegradation behavior of the epoxy system DGEBA ($n = 0$)/1,2 DCH modified with different concentrations of the reactive diluent VCHD was studied by TGA. Analysis of experimental results suggests that in the conversion range studied, 20–35%, the reaction mechanism is somewhere between the different types of phase boundary controlled reaction and random nucleation with two nuclei on the individual particle.

References

1. Ellis, B. Chemistry and Technology of Epoxy Resins, 1st ed.; Blackie Academic: UK, 1993.

2. Núñez, L.; Fraga, F.; Fraga, L.; Rodríguez, J. A. J Therm Anal 1996, 47, 743.

3. Hatakeyama, T.; Quinn, F. X. Thermal Analysis: Fundamentals and Applications to Polymer Science; Ed.; Wiley: Chichester, UK, 1994.

4. Criado, J. M.; Málek, J.; Ortega, A. Thermochim Acta 1989, 147, 377.

5. Montserrat, S.; Málek, J.; Colomer, P. Thermochim Acta 1998, 313, 83.

6. Ma, S.; Hill, J. O.; Heng, S. J Therm Anal 1991, 37, 1161.

7. Sestak, J.; Berggren, G. Thermochim Acta 1971, 3, 1.

8. Kissinger, H. E. Anal Chem 1957, 29, 1702.

9. Flynn, J. H.; Wall, L. A. J Res Natl Bur Standards A, Phys Chem 1996, 70A, 487.

10. Ozawa, T. Bull Chem Soc, Jpn 1965, 38, 1881.

11. Coats, A. W.; Redfern, J. P. Nature 1965, 207, 290.

12. Van Krevelen, D. W.; Van Heerden, C.; Huntjons, F. J. Fuel 1951, 30, 253.

13. Horowitz, H. H.; Metzger, G. Anal Chem 1965, 35, 1464.

14. Senum, G. I.; Yang, K. T. J Therm Anal 1977, 11, 445.

15. Lee, H.; Neville, K. Handbook of Epoxy Resin; McGraw-Hill: New York, 1967.

16. May, C. A. Epoxy Resins: Chemistry and Technology; Marcel Dekker: New York, 1988.

17. Núñez, L.; Taboada, J.; Fraga, F.; Núñez, M. R. J Appl Polym Sci 1997, 66, 1377.

18. Jiménez, A.; Berenguer, V.; López, J.; Sanchez, A. J Appl Polym Sci 1993, 50, 1565.

19. Ozawa, T.; Kato, T. J Therm Anal 1991, 37, 1299.

20. Núñez, L.; Fraga, F.; Núñez, M. R.; Villanueva, M. Polymer 2000, 41, 4635.

21. Doyle, C. D. Nature 1965, 207, 240.